S. Eckert | P. S. Miedema | W. Quevedo | B. O'Cinneide | M. Fondell | M. Beye | A. Pietzsch | M. Ross | M. Khalil | A. Föhlisch

Molecular structures and protonation state of 2-Mercaptopyridine in aqueous solution

Suggested citation referring to the original publication:
Chemical Physics Letters 647 (2016) 103-106
DOI https://doi.org/10.1016/j.cplett.2016.01.050
ISSN (print) 0009-2614
ISSN (online) 2590-1419

Chemical Physics Letters 647 (2016) 103–106

Contents lists available at ScienceDirect

Chemical Physics Letters

journal homepage: www.elsevier.com/locate/cplett

Molecular structures and protonation state of 2-Mercaptopyridine in aqueous solution

S. Eckert[a,b,*], P.S. Miedema[a], W. Quevedo[a], B. O'Cinneide[a], M. Fondell[a], M. Beye[a], A. Pietzsch[a], M. Ross[c], M. Khalil[c], A. Föhlisch[a,b]

[a] Institute Methods and Instrumentation in Synchrotron Radiation Research, Helmholtz-Zentrum Berlin für Materialien und Energie GmbH, Albert-Einstein-Str. 15, 12489 Berlin, Germany
[b] Institut für Physik und Astronomie, Universität Potsdam, Karl-Liebknecht-Str. 24/25, 14476 Potsdam, Germany
[c] Department of Chemistry, University of Washington, 36 Bagley Hall, Seattle, WA 98195, USA

ARTICLE INFO

Article history:
Received 23 November 2015
In final form 19 January 2016
Available online 25 January 2016

ABSTRACT

The speciation of 2-Mercaptopyridine in aqueous solution has been investigated with nitrogen 1s Near Edge X-ray Absorption Fine Structure spectroscopy and time dependent Density Functional Theory. The prevalence of distinct species as a function of the solvent basicity is established. No indications of dimerization towards high concentrations are found. The determination of different molecular structures of 2-Mercaptopyridine in aqueous solution is put into the context of proton-transfer in keto-enol and thione–thiol tautomerisms.

1. Introduction

Among chemical reactions, proton-transfer processes are of prime importance in chemistry and biochemistry and refer to the smallest possible, yet ubiquitous chemical rearrangements that are vital to life. Keto-enol and thione-thiol tautomerisms are prototypes of such processes which are widely investigated. In particular, these tautomers have dynamic equilibria that depend on temperature, concentration and solvent [1–4]. Keto-enol tautomerism transfers hydrogen (H) between carbon and oxygen, while for thione–thiol tautomerisms the proton is exchanged between sulphur (S) and nitrogen (N) bonding partners.

Tautomeric equilibria have a significant impact on the definition of possible base pairs in DNA [5] and on DNA replication and mutation processes [6], for example. The amino acid cysteine is another prominent example highlighting the importance of tautomerism in biology. Its S-H building block can be activated by the thione–thiol interconversion. Two cysteine molecules with additional oxygen can form a disulfide bridge and water [7]. These bridges may contribute to protein tertiary or quaternary structure and play a significant role in defining a protein's biological function [8].

Compared to the above mentioned cysteine, 2-Mercaptopyridine (2-MP) is a simpler version of a tautomer and proton transfer compound, that still contains the two functional building blocks N-H and S-H. 2-MP can exist protonated at the N (thione) or S (thiol) atom. The presence of the thione and thiol form of 2-MP is known to depend on the physical state and solvent environment. In its gaseous form [9] as well as in non-polar solvents [10] the thiol 2-MP tautomer is present, whereas the thione form dominates in polar solvents [4,3,11–14]. In addition the dimerization of 2-MP via disulfide bridge formation has been reported, i.e. at the exposure to oxygen [15] and in the solid phase [16–18].

N 1s (K-edge) Near Edge X-ray Absorption Fine Structure (NEXAFS) spectroscopy has been shown to be a sensitive technique to directly probe the protonation states of molecular N-sites [19–22]. In this study we utilize the element specific and chemical state selective detection of the speciation of 2-MP with N K-edge NEXAFS spectroscopy, probing transitions between N 1s core levels and valence states with p-character. In combination with Time Dependent Density Functional Theory (TD-DFT) calculations the relevant species of 2-MP in aqueous solution are determined out of multiple structural states this cyclo-organic molecule can accommodate.

2. Results

Figure 1a provides the experimental NEXAFS spectra of aqueous 2-MP for different sample concentrations. Directly one can notice

* Corresponding author at: Institute Methods and Instrumentation in Synchrotron Radiation Research, Helmholtz-Zentrum Berlin für Materialien und Energie GmbH, Albert-Einstein-Str. 15, 12489 Berlin, Germany.
E-mail address: sebastian.eckert@helmholtz-berlin.de (S. Eckert).

http://dx.doi.org/10.1016/j.cplett.2016.01.050

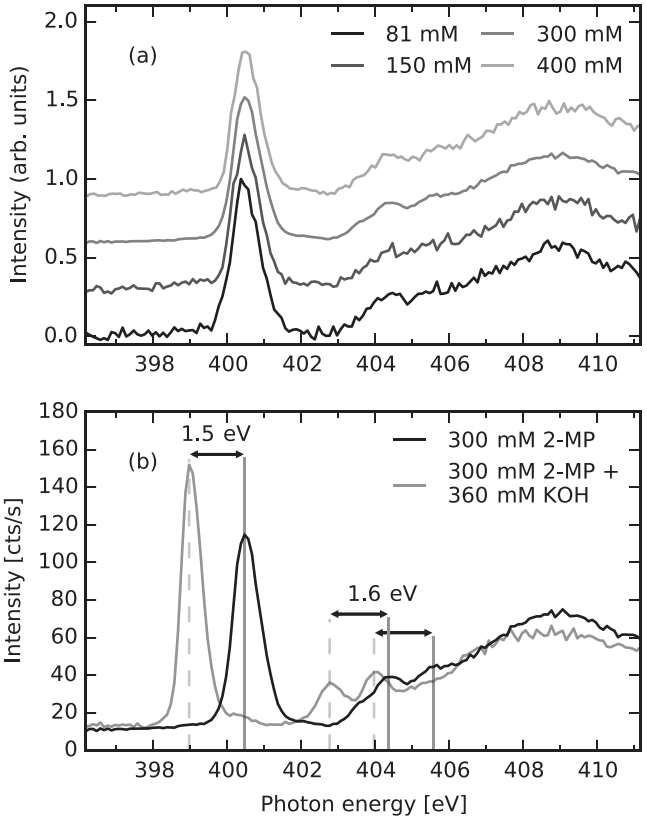

Figure 1. Near Edge X-ray Absorption Fine Structure at the N K-edge of 2-Mercaptopyridine (2-MP): (a) 2-MP in pure water as a function of concentration. Area normalized spectra. (b) 2-MP in pure water [2-MP] = 300 mM and in an alkaline aqueous solution [2-MP] = 300 mM, [KOH] = 360 mM.

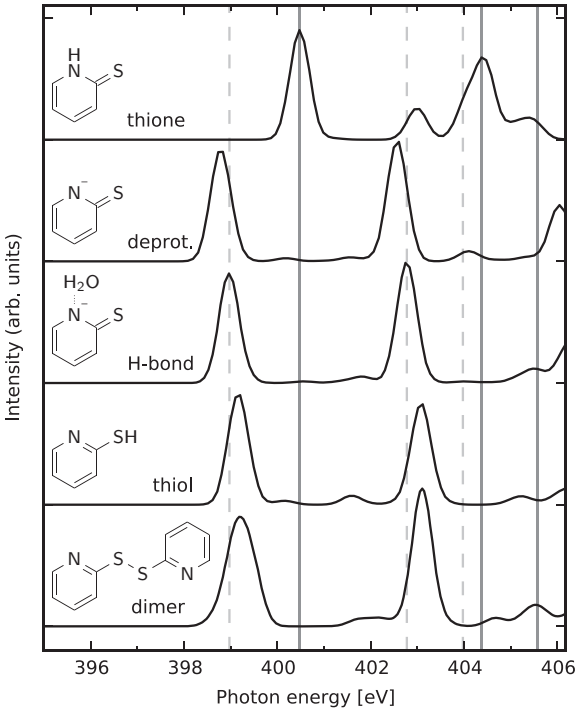

Figure 2. Calculated Near Edge X-ray Absorption Fine Structure of the N K-edge of 2-Mercaptopyridine. The energy position of the π^* resonance strongly depends strongly on the protonation state of the N-site in the molecular structures. Vertical lines indicate positions of experimental resonances from Figure 1b.

that the spectral shape is not influenced by the concentration in the studied regime of 81–400 mM 2-MP in water. The NEXAFS of 2-MP in an extreme basic environment as shown in Figure 1b exhibits a π^* absorption resonance shifted by 1.5 eV towards lower energies with respect to 2-MP in neutral solution. The KOH concentration in the basic solution exceeds the 2-MP concentration by a factor of 1.2. The spectral intensity in the range of the absorption resonance of 2-MP in a neutral environment at 400.5 eV is close to the background level.

Spectral features on top of the continuum (energies higher than 402 eV) are also shifted by the same amount towards lower energies as the π^* resonance for 2-MP in the basic environment (separation of solid and dashed vertical lines in Figure 1b.

To interpret the spectral differences depicted in Figure 1 we performed TD-DFT calculations to determine the N K-edge X-ray absorption cross section for the thione, thiol, deprotonated and dimer molecular structures of 2-MP as shown in Figure 2. The calculations are based on the 2-MP species in a purely molecular representation without solvent molecules. The calculated transitions can directly be assigned to experimentally detected bound state excitations. Positions of maxima in the measured NEXAFS spectra in Figure 1 are marked with vertical lines in Figure 2. Above the ionization threshold the additional continuum contributions have not been considered computationally, since they only cause an additional structureless contribution as visible in the experimental data in Figure 1 above 402 eV. All species exhibit a strong π^* absorption resonance for photon energies below 402 eV. The simulated spectrum for the thione form shows a π^* absorption resonance at 400.5 eV whereas the other considered species exhibit the resonance around 399 eV. This observation can be understood in a molecular orbital picture: the presence of a proton near the N-site increases the energetic splitting of bonding and anti-bonding orbitals and therefore the π^* absorption resonance appears at higher energies for the thione form. The calculated spectra were normalized to the height of the π^* resonance and neither the relative intensities nor the photon energies of the second sharp resonance at roughly 402.9 eV differ significantly between the thiol, the deprotonated and the dimer form of 2-MP. The NEXAFS calculations for the thione species predict strong X-ray absorption cross sections at energies correlated with spectral features of 2-MP in a neutral environment (solid vertical lines in Figure 2). We conclude that the thione species of 2-MP is dominant in the regime of submolar concentrations in water. Experimentally detected transitions for 2-MP in a basic surrounding (dashed vertical lines in Figure 2) overlap well with the resonances predicted for the H-bond species, resembling a 2-MP molecule which coordinates with an OH^- ion. This configuration is equivalent to the coordination of the deprotonated 2-MP species with a solvent molecule. Hence, deprotonation of the molecular N-site in 2-MP can be visualized using NEXAFS spectroscopy.

The different intensity ratios between the prominent transitions when comparing experimental and calculated spectra can originate from the neglect of the continuum in the calculations. In addition, the experimental NEXAFS is detected by its partial fluorescence yield which is known to deviate slightly in relative peak heights from the calculated cross sections [28].

Our findings are in agreement with the established 'building block approach', where molecular moieties determine NEXAFS spectral features [29]. The molecular TD-DFT calculations show good agreement with the experimental data in a single molecule approach. Therefore, we deduce that the valence electronic structure at the N-site of 2-MP is dominantly influenced by the coordination of its closest binding partners. Our data do not exhibit any indication for intermolecular coordination of multiple 2-MP molecules in the investigated chemical environments. Our assignment of the experimentally detected shift of the π^* resonance

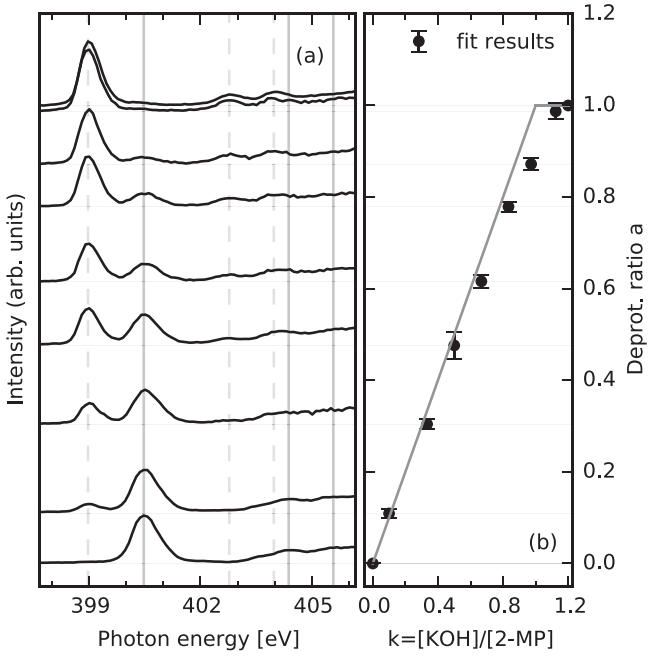

Figure 3. The balance of protonation and deprotonation of 2-Mercaptopyridine [2-MP (aq)] as a function of k=[2-MP]/[KOH]: (a) Near Edge X-ray Absorption Fine Structure of the N K-edge with π^* states of protonated and deprotonated 2-MP. (b) 2-MP deprotonation ratio at different relative concentrations k extracted from spectra in (a). A linear dependence motivated by a kinetic model of direct coordination between the 2-MP and the OH^- molecules is plotted to guide the eye.

for protonated and deprotonated N differs from the approach by Thomason et al. in which intermolecular interactions were introduced in the calculations in order to reproduce this experimental finding in imidazole [22].

Having identified the different 2-MP N-site protonation states in the N K-edge NEXAFS, we proceed with a detailed investigation of the 2-MP molecular structure as function of the concentration of potassium hydroxide (KOH) (Figure 3). The NEXAFS spectra for different relative concentrations k between 2-MP and KOH

$$k = \frac{[\mathrm{KOH}]}{[2-\mathrm{MP}]}$$

are presented in Figure 3a. For increasing k, the strong π^* resonance at 400.5 eV decreases in intensity, while at the same time a feature at 399 eV appears for $k>0$ and increases with k. As these spectral signatures were identified as resonances of the protonated (thione) and deprotonated species respectively, the changes in NEXAFS spectra with increasing k are interpreted as a gradual species transformation. A superposition of the spectral intensity (I) of the two extreme cases from Figure 1b

$$(1-a)\,I_{2-\mathrm{MP}} + a\,I_{2-\mathrm{MP+KOH}}$$

is fitted to the experimental data. In this way the 2-MP deprotonation ratio a is extracted from the spectra for different k. The extracted ratios are shown in Figure 3b. The spectral ratio of the two species has a linear relationship to the concentration ratio k, indicating direct coordinative influence of OH^- ions on the protonation state of 2-MP in aqueous solution.

3. Conclusion

The thione tautomer of 2-MP has been clearly determined as predominant species in aqueous solution with N K-edge NEXAFS and TD-DFT. Other molecular structures that 2-MP is known to exhibit in different environments have been excluded through the distinct spectral signatures and chemical state selectivity of our combined approach. Motivated by the omnipresence of tautomerism in nature, we establish the signature of N-site (de)protonation and the associated building blocks for biologically relevant molecules. In the future, applying N K-edge NEXAFS to amino acids or even proteins, the building block aspect of NEXAFS spectroscopy [29] could be used to disentangle the differently protonated N-sites in the same molecule to establish their structure-function relationship.

4. Materials and methods

The experimental data were acquired in the liquid flexRIXS experiment [23] at the beam line U49-2_PGM-1 of the synchrotron Bessy II (Helmholtz-Zentrum Berlin). The used sample was 2-Mercaptopyridine (2-MP) with a purity of 99% supplied by Sigma–Aldrich, Germany. For every shift of the beamtime the 2-MP solution was prepared freshly dissolving it in deionized water. It was degassed and sprayed into the experimental high vacuum chamber within a liquid jet. It had a diameter of 20 μm and was run with a JASCO High-Performance Liquid Chromatography (HPLC) pump. The total jet flow was 0.5 ml per minute. The 2-MP and the OH^- concentration in the sample solution was varied using a mixer unit of the HPLC-pump. The dissolved sample was excited with horizontally polarized X-ray photons at the Nitrogen (N) 1s (K-edge) absorption resonance. The bandwidth of the incidence radiation was 250 meV. The photon energy was calibrated utilizing K-edge absorption lines of N gas. Drifts of the monochromator were compensated by comparisons of 300 mM 2-MP (aq) spectra measured at different days. We detected the photon energy dependent partial fluorescence yield of the sample in a 90° scattering geometry as a measure of Near Edge X-ray Absorption Fine Structure (NEXAFS) signal. The soft X-ray emission spectrometer Scienta XES 350 [24] was utilized for that purpose. The emission spectrum was integrated between 370 and 420 eV, including all detected N valence emission features. The experimental accuracy is limited by the 250 meV incidence energy beamline resolution and the stepwidth of 100 meV in the recorded data.

Density Functional Theory calculations were performed with the ORCA package [25]. First, the geometries of all molecules were optimized with the BP86 exchange correlation functional and DEF2-TZVP basis sets [26]. Subsequently, the geometry optimized structures were used in Time Dependent Density Functional Theory to generate N K-edge X-ray absorption spectra [27] with a broadening of 0.5 eV. The energy axis of the calculated thione species spectrum was shifted to the experimental spectrum of 2-MP in water. All other calculated spectra were shifted equally.

Acknowledgements

We thank HZB for the allocation of synchrotron radiation beamtime. Technical support by Christian Weniger is acknowledged. We acknowledge the European Research Council for funding the Open Access of this article. MB thanks the Volkswagen-Stiftung for financial support. MR and MK acknowledge the support of the David and Lucile. Packard Fellowship for Science and Engineering. Graphics were generated using the Matplotlib package [30].

References

[1] P. Beak, J.B. Covington, S.G. Smith, J. Am. Chem. Soc. 98 (1976) 8284.
[2] P. Beak, F.S. Fry, J. Lee, F. Steele, J. Am. Chem. Soc 98 (1976) 171.
[3] P. Beak, J.B. Covington, S.G. Smith, J.M. White, J.M. Zeigler, J. Org. Chem. 45 (1980) 1354.
[4] P. Beak, Acc. Chem. Res. 10 (1977) 186.
[5] J.D. Watson, F.H.C. Crick, Nature 171 (1953) 737.
[6] J. Florián, J. Leszczyński, J. Am. Chem. Soc. 118 (1996) 3010.
[7] J.A. Schellman, The Stability of Hydrogen-bonded Peptide Structures in Aqueous Solutions, Comptes rendus des travaux du Laboratoire Carlsberg Série

chimique: Comptes rendus des travaux du Laboratoire Carlsberg; Hagerup in Komm, 1955.
[8] M. Sela, S. Lifson, Biochim. Biophys. Acta 36 (1959) 471.
[9] M.J. Nowak, L. Lapinski, H. Rostkowska, A. Les, L. Adamowicz, J. Phys. Chem. 94 (1990) 7406.
[10] P. Beak, J.B. Covington, J.M. White, J. Org. Chem. 45 (1980) 1347.
[11] P. Beak, J.B. Covington, J. Am. Chem. Soc. 100 (1978) 3961.
[12] A.R. Katritzky, K. Jug, D.C. Oniciu, Chem. Rev. 101 (2001) 1421.
[13] M.W. Wong, K.B. Wiberg, M.J. Frisch, J. Am. Chem. Soc. 114 (1992) 1645.
[14] R. Du, C. Liu, Y. Zhao, K.-M. Pei, H.-G. Wang, X. Zheng, M. Li, J.-D. Xue, D.L. Phillips, J. Phys. Chem. B 115 (2011) 8266.
[15] S. Stoyanov, T. Stoyanova, P.D. Akrivos, P. Karagiannidis, P. Nikolov, J. Heterocycl. Chem. 33 (1996) 927.
[16] B.R. Penfold, Acta Crystallogr. 6 (1953) 707.
[17] U. Ohms, H. Guth, A. Kutoglu, C. Scheringer, Acta Crystallogr. Sect. B: Struct. Crystallogr. Cryst. Chem. 38 (1982) 831.
[18] V. Martínez-Merino, M.J. Gil, J. Chem. Soc. Perkin Trans. 2 (2) (1999) 801.
[19] J. Hasselström, A. Föhlisch, O. Karis, N. Wassdahl, M. Weinelt, A. Nilsson, M. Nyberg, L.G.M. Pettersson, J. Stöhr, J. Chem. Phys. 110 (1999) 4880.
[20] M. Nyberg, J. Hasselström, O. Karis, N. Wassdahl, M. Weinelt, A. Nilsson, L.G.M. Pettersson, J. Chem. Phys. 112 (2000) 5420.
[21] J. Hasselström, O. Karis, M. Weinelt, N. Wassdahl, A. Nilsson, M. Nyberg, L. Pettersson, M. Samant, Stöhr, J. Surf. Sci. 407 (1998) 221.
[22] M.J. Thomason, C.R. Seabourne, B.M. Sattelle, G.A. Hembury, J.S. Stevens, A.J. Scott, E.F. Aziz, S.L.M. Schroeder, Faraday Discuss. 179 (2015) 269.
[23] K. Kunnus, et al., Rev. Sci. Instrum. 83 (2012) 123109.
[24] J. Nordgren, G. Bray, S. Cramm, R. Nyholm, J.-E. Rubensson, N. Wassdahl, Rev. Sci. Instrum. 60 (1989) 1690.
[25] F. Neese, Wiley Interdiscip. Rev. Comput. Mol. Sci. 2 (2012) 73.
[26] F. Weigend, R. Ahlrichs, Phys. Chem. Chem. Phys. 7 (2005) 3297.
[27] C.J. Pollock, S. DeBeer, J. Am. Chem. Soc. 133 (2011) 5594.
[28] P.S. Miedema, P. Wernet, A. Föhlisch, Phys. Rev. A 89 (2014) 052507.
[29] J. Stöhr, Book, vol. 25, Springer Series in Surface Sciences; Springer Berlin Heidelberg, Berlin, Heidelberg, 1992, pp. xv, 403.
[30] J.D. Hunter, Comput. Sci. Eng. 9 (2007) 90.